A spatial bio-economic modelling approach on the trade-offs between global bioenergy demand, agricultural intensification, expansion, and trade

Hermann Lotze-Campen, Alexander Popp, Tim Beringer, Christoph Müller, Wolfgang Lucht

Affiliations (all authors):

Potsdam Institute for Climate Impact Research (PIK),
PO Box 60 12 03, 14412 Potsdam, Germany

Corresponding author:

Hermann Lotze-Campen, Tel. +49-331-2882699,
Fax +49-331-288 2620, E-mail: lotze-campen@pik-potsdam.de

Contributed Paper prepared for presentation at the International Association of Agricultural Economists Conference, Beijing, China, August 16-22, 2009

Abstract

Increased future demands for food, fibre and fuels from biomass can only be met if the available land and water resources on a global scale are used and managed as efficiently as possible. The main routes for making the global agricultural system more productive are through intensification and technological change on currently used agricultural land, land expansion into currently non-agricultural areas, and international trade in agricultural commodities and processed goods. In order to analyse the trade-offs and synergies between these options, we present a global bio-economic modelling approach with a special focus on spatially explicit land and water constraints as well as technological change in agricultural production. For a given bioenergy demand scenario until the middle of the 21st century and different land allocation options, we analyse the required rate of productivity increase on agricultural land as well as the implicit values (shadow prices) of limited land and water resources. The shadow prices for bioenergy are provided as a metric for assessing the trade-offs between different land allocation options.

Keywords: Land use change, Spatial modelling, Technological change

1. Introduction

Over the next decades, the competition for scarce land and water resources will further intensify, due to rising global population and wealth on the demand side, and due to changing climate conditions on the supply side. Furthermore, ambitious policies for climate change mitigation will increase the pressure on agricultural production, as part of the global energy supply for human purposes will be provided by various kinds of biomass as a primary energy carrier. The market and price effects on agriculture based on increased bioenergy demand may be even bigger than the direct climate impacts on agricultural productivity. Recent estimates on the potential global bio-energy supply range from less than 100 EJ/year to over 400 EJ/year for 2050 (e.g. Berndes et al. 2003, Hoogwijk 2004). These estimates differ due to large discrepancies in land availability for biomass plantations and yield levels in crop production. However, concerns about the sustainability of bioenergy due to potentially unfavourable net greenhouse gas balances have also been raised (e.g. Crutzen et al. 2007, Searchinger et al. 2008, Fargione et al. 2008). Finally, the need for biodiversity conservation on a global scale will increase the demand for certain shares of the land to be used less intensively or taken out of production altogether.

While the combined impacts of all these trends are still highly uncertain, approaches to future land-use management will be confronted with serious trade-offs. If more land is to be taken out of production, intensity on the remaining land has to be increased. Both increased land-use intensity and land expansion into new areas may entail higher greenhouse gas emissions from the agricultural sector. The challenge of analyzing these trade-offs and projecting future land-use patterns is to account, within one modelling framework, for the socio-economic determinants of agricultural demand as well as for the spatial heterogeneity of the land's suitability for agricultural production.

As a metric for weighing conflicting goals in large-scale land use decisions we choose the required rate of technological change (or productivity increase) to fulfil global food, fibre and bioenergy demand under different constraints on land availability and trade. As additional technological change will only be provided at additional costs of production (through investment or research and development), we also translate this into increased costs of production. Our modelling approach enables us to translate various biophysical constraints to agricultural production into relevant production costs, and through derived shadow prices it also provides a quantitative measure of scarcity for land and water resources.

In this study we focus on the main routes for making the global agricultural system more productive: (i) intensification and technological change, (ii) land expansion into currently non-agricultural areas, and (iii) international trade in agricultural commodities and processed goods.

2. Linking an economic land-use allocation model to a process-based vegetation-hydrology model

We have developed a mathematical programming approach, which is coupled to a grid-based dynamic vegetation model, to simulate spatially explicit land-use and water-use patterns. This approach provides most flexibility to integrate various types of biophysical constraints into an economic decision-making process. It provides a straightforward way to link monetary and physical units and processes. Instead of using empirically based, but rather static yield functions, potential crop productivity and related water use is explicitly modelled. The dual solution of the mathematical programming model provides valuable insights into the internal use value of resource constraints. The model computes shadow prices for binding constraints in specific grid cells, e.g. in this case related to land and water availability, reflecting the amount a land manager would be willing to pay for relaxing the constraint by one unit.

Our globally applicable land-use model MAgPIE is a non-linear programming model with a focus on agricultural production, land and water use. The information flow in our coupled modelling approach is shown in Figure 1.

[Insert Figure 1 about here]

The linear objective function of the land-use model is to minimize total cost of production for a given amount of regional food and bioenergy demand. Regional food energy demand is defined for an exogenously given population in ten food energy categories (cereals, rice, vegetable oils, pulses, roots and tubers, sugar, ruminant meat, non-ruminant meat, and milk), based on regional diets (FAOSTAT, 2004). Food and feed energy for the ten demand categories can be produced by 20 cropping activities (temperate cereals for food or feed, maize for food or feed, tropical cereals for food or feed, rice, five oil crops, pulses, potatoes, cassava, sugar beets, sugar cane, vegetables/fruits/nuts, two fodder crops) and 3 livestock activities (ruminant meat, non-ruminant meat, milk). Feed for livestock is produced as a mixture of grain, green fodder, and pasture at fixed proportions. Fibre demand is currently fulfilled with one cropping activity (cotton). Cropland, pasture and irrigation water are fixed inputs in limited supply in each grid cell, measured in physical units of hectares (ha) and cubic meters (m^3). Variable inputs of production are labour, chemicals, and other capital (all measured in US$), which are assumed to be in unlimited supply to the agricultural sector at a given price. Moreover, the model can endogenously decide to acquire yield-increasing technological change at additional costs, if otherwise there is no feasible solution (i.e. land use pattern) under a given set of resource constraints.

For future projections the model works on a time step of 10 years in a recursive dynamic mode. The link between two consecutive periods is established through the land-use pattern. The optimized land-use pattern from one period is taken as the initial land constraint in the next. If necessary, additional land from the non-agricultural area can be converted into cropland at additional costs.

Potential crop yields for each grid cell are supplied by the Lund-Potsdam-Jena dynamic global vegetation model with managed Lands (LPJmL) (Sitch et al., 2003; Bondeau et al., 2007). In addition to major food and feed crops, also cellulose-based bioenergy crops have been implemented. LPJmL endogenously models the dynamic processes linking climate and soil conditions, water availability and plant growth, and takes the impacts of CO_2, temperature and radiation on yield directly into account. LPJmL also covers the full hydrological cycle on a global scale, which is especially useful as carbon and water-related processes are closely linked in plant physiology (Gerten et al., 2004; Rost et al., 2008). Standard LPJmL outputs include changes in net primary production and different fractions of biomass, changes in carbon pools and water balances.

Spatially explicit data on yield levels and freshwater availability for irrigation is provided on a regular geographic grid, with a resolution of three by three degrees, dividing the terrestrial land area into 2178 discrete grid cells of an approximate size of 300 km by 300 km at the equator. Each cell of the geographic grid is assigned to one of ten economic world regions: Sub-Saharan Africa (AFR), Centrally-planned Asia including China (CPA), Europe including Turkey (EUR), the Newly Independent States of the Former Soviet Union (FSU), Latin America (LAM), Middle East/North Africa (MEA), North

America (NAM), Pacific OECD including Japan, Australia, New Zealand (PAO), Pacific (or Southeast) Asia (PAS), and South Asia including India (SAS). The regions are initially characterized by data for the year 1995 on population (CIESIN et al., 2000), gross domestic product (GDP) (World Bank, 2001), food energy demand (FAOSTAT, 2004), average production costs for different production activities (McDougall, 1998), and current self-sufficiency ratios for food (FAOSTAT, 2005). While all supply-side activities in the model are grid-cell specific, the demand side is aggregated at the regional level. Aggregate demand within each region, defined by total population, average income and net trade, is being met by the sum of production from all grid cells within the region.

Trade in food products between regions is simulated endogenously, constrained by minimum self-sufficiency ratios for each region. This is to say that some minimum level of domestic demand has to be produced within the region, while the rest can be allocated to other regions according to comparative advantages. If, for instance, a region currently has a self-sufficiency ratio of 1.2 for a certain product, then in future projections this may either be kept constant or gradually reduced over time to account for global trade liberalization.

Land conversion activities provide for potential expansion and shifts of agricultural land in specific locations. For the base year 1995, total agricultural land is constrained to the area currently used within each grid cell, according to Ramankutty and Foley (1999). However, if additional land is required for fulfilling demand, this can be taken from the pool of non-agricultural land at additional costs. These land-conversion costs force the model to utilize available cropland first, and land conversion will become relevant only if land becomes scarce in a certain location or if the marginal cost reductions by producing crops on converted land outweigh the costs of conversion. LPJmL computes trends in potential crop yields and irrigation water requirements for the 20th and 21st century, taking climate change impacts into account (Bondeau et al., 2007). Under plausible scenarios of population and income growth, MAgPIE calculates food and bioenergy demand and allows for future projections of spatially explicit land-use patterns, for deriving future technological change rates, and for valuating constraints on land and water availability or trade restrictions.

Bioenergy in MAgPIE is supplied as a mix of three different types: vegetable-oil-based from various oil crops, starch/sugar-based from cereals and sugar crops, and cellulose-based from specialized grassy and woody bioenergy crops. Demand is currently not specified according to different uses in the energy system, e.g. heating, fuels etc.. All bioenergy products in the model are delivered into an aggregated demand pool. Future trends in food demand are computed as a function of GDP per capita based on a cross-country regression.

3. Global bioenergy demand in 2055 under different scenarios of intensification, land expansion, and international trade

We apply our modelling system to a modest future bioenergy scenario with three different land allocation options. Besides changes in population, economic growth and environmental production conditions, the issue of technological change in production (i.e. yield increase) is of crucial importance for the resulting spatial patterns of land and water use. This can be tackled in two directions. With most other modelling approaches, this is done by assuming a future trend in productivity growth and then deriving the economic and environmental consequences. In contrast, with the mathematical programming model presented here, the issue can be turned around, and the minimum rate of technological change required to meet certain constraints can be derived. Hence, the main question behind the scenarios described here is: "How much yield increase (or technological change) is required to fulfill future global demand for bioenergy and food under different restrictions on land and water use?"

We run the MAgPIE model in six 10-year time steps from 1995 until 2055 in a recursive dynamic manner. The model is driven by external scenarios on population growth and GDP growth taken from the SRES A2 scenario (IPCC, 2000). Global population increases up to about 9 billion in the year 2055, and average world income per capita reaches about 15,000 US$ (in 1995 purchasing power parity terms). Global bioenergy demand is determined exogenously, starting close to zero in 1995 and reaching about 100 ExaJoule in 2055. This is a hypothetical scenario with share of about 10 percent in total primary energy consumption in 2055. It is rather modest, compared to other studies on global bioenergy potential. Here the demand scenario serves as an example to demonstrate the type of trade-off analyses to be conducted with our modelling approach. In principle, any bioenergy demand path (global or with regional resolution) can be implemented in the same way. Figure 2 provides an overview of input data for the scenarios in this paper.

[Insert Figure 2 about here]

Scenarios

Our baseline scenario covers only food demand and keeps the cropland area constant over time. Regional trade balances are also kept constant at 1995 levels. The baseline results provide a benchmark for the minimum technological change rates which are required to achieve future food and feed demand without any land expansion into currently non-agricultural areas. The scenario Biof100 adds a bioenergy demand path, as described in Figure 2, to the baseline conditions, i.e. again without land expansion. The scenario Biof100+area allows for area expansion together with bioenergy demand. In each time step, a maximum of 1% of initially non-agricultural land is allowed to be converted into cropland in each grid cell. And finally, the scenario Biof100+trade keeps the cropland area constant, but allows for increased trade of food, feed and bioenergy between the 10 regions. This is implemented by lowering the minimum self-sufficiency rate for each region, which leads to a higher share of production being allocated to the most productive grid cells on a global scale.

Technological change rates

The resulting rates of technological change for the baseline and the three bioenergy scenarios are provided in Figure 3. The model results are compared with FAO statistics from the period 1970-1995. The numbers describe average regional yield increases per year for all crops over a given period (1995-2055 for the future scenarios).

[Insert Figure 3 about here]

Under our chosen baseline conditions on population growth, income growth, and no cropland expansion, average global crop yields need to increase by about 0.9 percent per year until the middle of the century. This is significantly lower than the trend over the last three decades. In most regions the required future rate of change is lower than the observed rate in the past, except for AFR and FSU. For AFR this reflects rather slow productivity increase in the past, and the expected effects of strong growth in population and income in the future. In FSU the low rate in the past is due to the breakdown of production in the transition period of the 1980s and 1990s. Very low future rates in EUR and PAO are mainly due to expected slow population growth (or even decline) in these regions.

In the Biof100 scenario, without land expansion, the rate of technical change increases significantly, however, in all regions except AFR and FSU it remains below historical rates of productivity increase. The weighted average rate for the world as a whole is close to the historical rate of 1.3 percent per year. In the area expansion scenario (Biof100+area) the required rate of technological change is about the same as in the baseline. This indicates that in 2055 100 ExaJoule of primary bioenergy can be produced without major implication for the food system, if recently observed technology trends can be maintained over the next decades. The scenario with increased trade (Biof100+trade) shows a mixed picture. One would expect that, due to more flexibility in land allocation across the globe, average technological change rates should be lower than in the scenario Biof100. In fact, in all regions except AFR and FSU this is the case. In contrast, yield increase is much higher in AFR and FSU. Since these are the "low-cost" regions in the model (including the costs of technological change), with increased trade the model shifts as much production as possible into these regions. The resulting weighted average global technological change rate is at the same level as in the Biof100 scenario without trade. However, it is interesting to note that total costs of production, which are not shown here, are significantly lower with increased trade, showing one important trade-off to be taken into account.

Land expansion

Figure 4 shows the development of total cropland and the share of bioenergy crops in the three bioenergy scenarios. The same amount of 100 ExaJoule bioenergy in 2055 is produced on the smallest area in the trade scenario. This illustrates the effect of more efficient land allocation across the globe.

[Insert Figure 4 about here]

Shadow prices for water

Figure 5 shows the implicit value of irrigation water in each grid cell, as derived by the model for the Biof100 scenario in 2005 and 2055. This is a quantitative economic measure of resource scarcity, as in an optimization model the shadow price would be zero for any constraint that is non-binding in the solution.

[Insert Figure 5 about here]

The upper map highlights areas where the model indicates water scarcity in 2005. The second map shows that water scarcity increases and that many new grid cells become water-scarce over time due to increased demand from food and bioenergy production. Grid cells with the highest shadow prices indicate where water-saving methods and technologies could be applied with the highest economic benefit. The shadow price indicates, by how much production costs would decrease if one additional cubic meter of water would be available in a specific location.

Shadow prices for bioenergy

As a final set of results, we show the shadow price for bioenergy in the model. Since the model minimizes production costs for a given demand for food and bioenergy products, these numbers show the marginal increase in production costs for an additional unit of output. This can also be interpreted as the minimum price that "the energy system" would have to pay for one additional unit of bioenergy.

[Insert Figure 6 about here]

While the shadow price for bioenergy is continuously rising in the Biof100 and Biof100+area scenarios, the curve has a different shape with increased trade. The strong increase in technological change in AFR and FSU seems to drive up production costs in the beginning, while the advantages of improved allocation dominate in later periods with higher bioenergy demand. In the end, the trade scenario shows the most efficient of all three global production patterns for bioenergy.

4. Conclusions

The model MAgPIE computes spatially explicit land-use and water-use patterns with global coverage by combining socio-economic information on population, income, food demand and production costs with spatially explicit environmental data on potential crop yields and water availability for irrigation. The structure of MAgPIE facilitates an integrated environmental-economic assessment. It provides essential inputs for assessing the trade-offs between different land-use options and economic as well as spatially disaggregated ecological constraints. The derived shadow prices provide a useful measure of scarcity and allow for an economic valuation of biophysical goals and constraints. This is unique in globally applicable land-use models, especially as MAgPIE explicitly considers water as an essential input to agricultural production. The demand for bioenergy has been included as an additional driving force for global land use change. This has been combined with different scenarios on land availability and expanded international trade.

In our baseline scenario, covering only food and feed demand, required future technological change rates are slightly lower than over the past decades. Furthermore, we conclude that 100 ExaJoule of primary bioenergy can be produced in 2055 without further land expansion, if technological change rates can be maintained at recent levels. If, at the same time, cropland is expanded into currently underused areas, required yield increases are substantially lower. Under a scenario of increased trade in agricultural and bioenergy products, a larger share of global production in the model is shifted to Sub-Saharan Africa and the Former Soviet Union, the regions with highest potential for low-cost productivity increases.

Our model does not only provide the opportunity to investigate the global biophysical potential for bioenergy production. It also assigns a shadow price to bioenergy output, depending on the level of demand and different constraints to land and water availability. This opens up a unique spectrum of all kinds of trade-off analyses between different scenarios, as it provides an economic metric and an aggregate measure for comparing different scenario outcomes. It also provides a method for valuation of biophysical resource, for which in most regions only imperfect markets or no markets at all exist. This type of land and water use model can establish a crucial link between economic and energy system models on the one hand, and process-based models on carbon and water cycles and other ecological processes on the other.

5. References

Berndes, G. et al. (2003) The contribution of biomass in the future global energy supply: a review of 17 studies. Biomass Bioenergy 25, 1–28

Berndes, G., Hoogwijk, M., van den Broek, R. (2003): The contribution of biomass in the future global energy supply: a review of 17 studies. Biomass and Bioenergy 25:1-28.

Bondeau, A., Smith, P., Zaehle, S., Schaphoff, S., Lucht, W., Cramer, W., Gerten, D., Lotze-Campen, H., Müller, C., Reichstein, M. and Smith, B., 2007. Modelling the role of agriculture for the 20th century global terrestrial carbon balance. Global Change Biology, 13(3): 679-706.

CIESIN, IFPRI and WRI, 2000. Gridded Population of the World (GPW), Version 2. Center for International Earth Science Information Network (CIESIN) Columbia University, International Food Policy Research Institute (IFPRI) and World Resources Institute (WRI), Palisades, NY.

Crutzen, P.J. et al. (2007) N2O release from agro-biofuel production negates global warming reduction by replacing fossil fuels. Atmos. Chem. Phys. Discuss. 7, 11191–11205

Döll, P. and Siebert, S., 2000. A digital global map of irrigated areas. ICID Journal, 49(2): 55-66.

FAOSTAT, 2004. Food Balance Sheets. Rome, FAO.

FAOSTAT, 2005. http://faostat.fao.org/ [Accessed: March, 2005].

Fargione, J., Hill, J., Tilman, D., Polasky, S., Hawthorne, P. (2008): Land Clearing and the Biofuel Carbon Debt. Science 319: 1235-1238.

Gerten, D., Schaphoff, S., Haberlandt, U., Lucht, W. and Sitch, S., 2004. Terrestrial vegetation and water balance - hydrological evaluation of a dynamic global vegetation model. Journal of Hydrology, 286(1-4): 249-270.

Hertel, T.W. (Ed.), 1997. Global trade analysis. Cambridge, Cambridge University Press.

Hoogwijk, M. (2004): On the global and regional potential of renewable energy sources. Ph.D. Dissertation. University of Utrecht, Netherlands.

IPCC, 2000. Special Report on Emissions Scenarios. IPCC.

Lee, H.L., Hertel, T., Sohngen, B., Ramankutty, N., 2005. Towards An Integrated Land Use Database for Assessing the Potential for Greenhouse Gas Mitigation, GTAP Technical Paper No. 25, West Lafayette, Indiana, USA.

McDougall, R.A., Elbehri, A. , Truong, T.P., 1998. Global Trade Assistance and Protection: The GTAP 4 Data Base. Center for Global Trade Analysis, Purdue University.

Ramankutty, N. and Foley, J., 1999. Estimating historical changes in global land cover: Croplands from 1700 to 1992. Global Biogeochemical Cycles, 13(4): 997-1027.

Rost, S.; Gerten, D.; Bondeau, A.; Lucht, W.; Rohwer, J.; Schaphoff, S. (2008): Agricultural green and blue water consumption and its influence on the global water system. Water Resources Research, online first. 10.1029/2007WR006331

Searchinger T., Heimlich R., Houghton R. A., Dong, Elobeid A., Fabiosa J., Tokgoz S., Hayes D., Tun-Hsiang Yu, 2008. Use of U.S. Croplands for Biofuels Increases Greenhouse Gases Through Emissions from Land-Use Change. Science 319: 1238-1242.

Sitch, S., Smith, B., Prentice, I., Arneth, A., Bondeau, A., Cramer, W., Kaplan, J., Levis, S., Lucht, W., Sykes, M., Thonicke, K. and Venevsky, S., 2003. Evaluation of ecosystem dynamics, plant geography and terrestrial carbon cycling in the LPJ dynamic global vegetation model. Global Change Biology, 9(2): 161-185.

World Bank, 2001. World Development Indicators (CD-ROM). Washington D.C.

6. Figure captions

Figure 1: Information flow within the coupled modeling system

Figure 2: Exogenous scenario inputs on regional population growth, regional growth in calorie intake per person per day, and global demand for bioenergy

Figure 3: Required annual yield increases (percent) over the period 1995-2055, baseline scenario plus scenarios with bioenergy, cropland expansion and trade (Simulation results, see text for further explanation). As a matter of orientation, the dashed line is set at 1.4 which is the rate of change equivalent to a doubling of yield in 50 years time.

Figure 4: Changes in total cropland and bioenergy areas for different bioenergy scenarios (million hectares) (Simulation results)

Figure 5: Shadow prices for irrigation water (US$/m3) in 2005 and 2055 (Simulation results)

Figure 6: Shadow price for bioenergy (US$/GJ) (Simulation results)

Figure 1

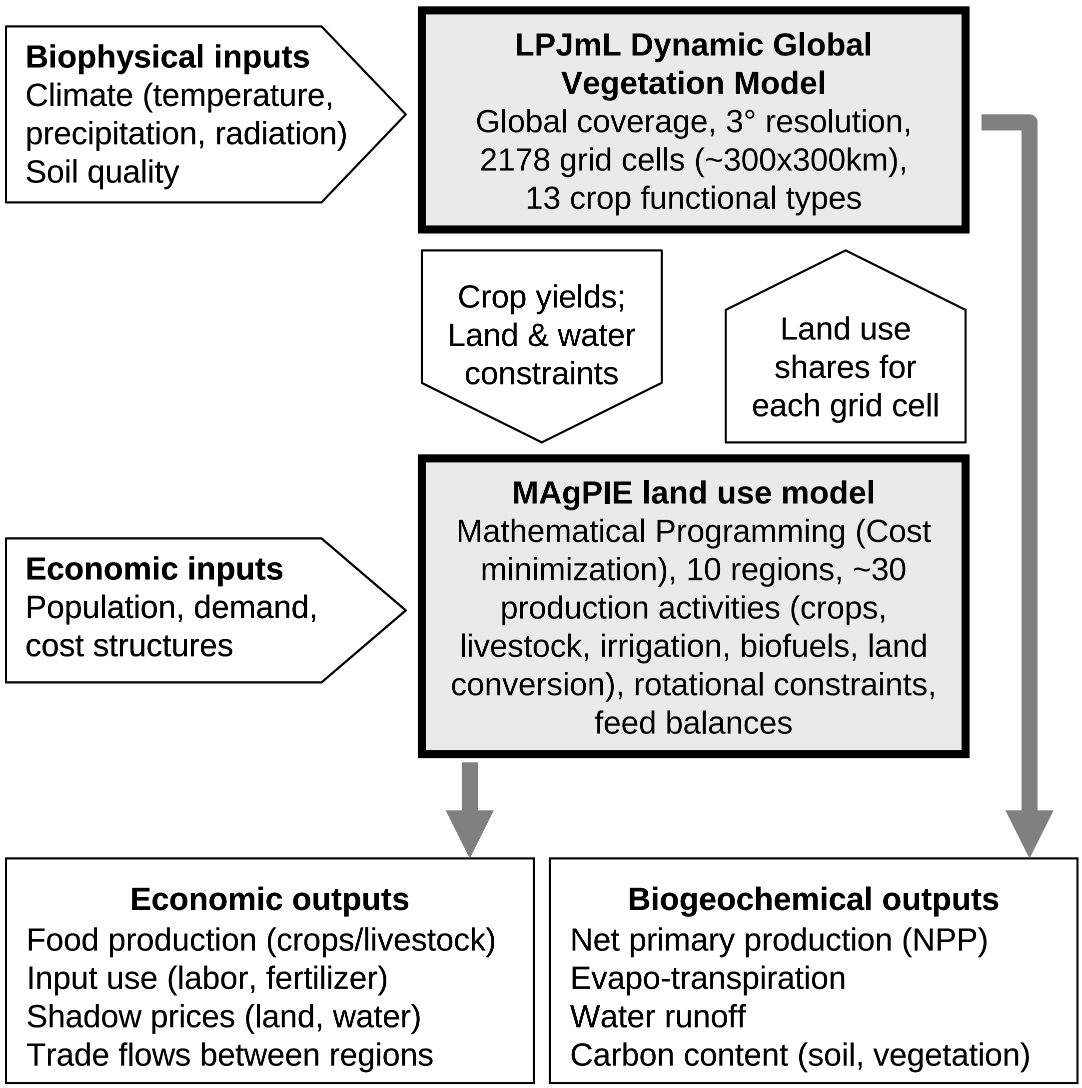
Biophysical inputs
Climate (temperature, precipitation, radiation)
Soil quality
LPJmL Dynamic Global Vegetation Model
Global coverage, 3° resolution, 2178 grid cells (~300x300km), 13 crop functional types
Crop yields; Land & water constraints
Land use shares for each grid cell
Economic inputs
Population, demand, cost structures
MAgPIE land use model
Mathematical Programming (Cost minimization), 10 regions, ~30 production activities (crops, livestock, irrigation, biofuels, land conversion), rotational constraints, feed balances
Economic outputs
Food production (crops/livestock)
Input use (labor, fertilizer)
Shadow prices (land, water)
Trade flows between regions
Biogeochemical outputs
Net primary production (NPP)
Evapo-transpiration
Water runoff
Carbon content (soil, vegetation)

Figure 2

Population (mio)	1995	2005	2015	2025	2035	2045	2055
World	5473	6525	7251	7903	8410	8797	9062
AFR	553	743	926	1125	1313	1481	1629
CPA	1281	1480	1582	1651	1673	1677	1659
EUR	554	589	586	575	559	532	505
FSU	276	293	295	295	285	275	262
LAM	452	550	623	687	739	780	810
MEA	278	357	423	486	541	590	633
NAM	292	332	355	375	391	400	404
PAO	134	146	148	147	146	144	140
PAS	383	462	517	565	614	652	674
SAS	1270	1572	1797	1998	2149	2265	2347
Food demand (kcal/capita/day)							
World	2615	2678	2745	2816	2892	2971	3054
AFR	2281	2345	2409	2476	2545	2615	2687
CPA	2533	2625	2720	2819	2921	3027	3137
EUR	3193	3257	3323	3389	3457	3526	3597
FSU	2565	2658	2754	2854	2957	3064	3175
LAM	2797	2871	2947	3026	3106	3188	3273
MEA	2692	2767	2844	2924	3006	3090	3177
NAM	3417	3473	3530	3588	3647	3707	3768
PAO	3309	3361	3415	3469	3524	3579	3636
PAS	2579	2667	2759	2854	2952	3054	3159
SAS	2272	2356	2443	2533	2626	2723	2823
Bioenergy demand (ExaJoule)							
World	4.4	7.8	13.2	21.9	36.2	59.9	99.4

Figure 3

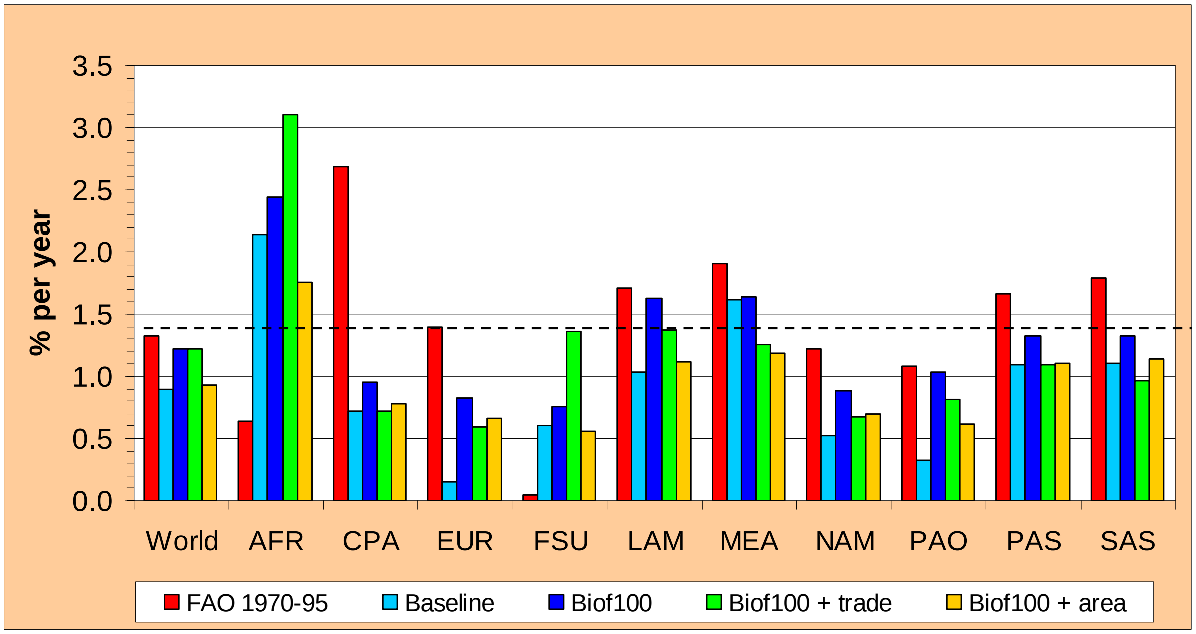
% per year
3.5
3.0
2.5
2.0
1.5
1.0
0.5
0.0
World
AFR
CPA
EUR
FSU
LAM
MEA
NAM
PAO
PAS
SAS
FAO 1970-95
Baseline
Biof100
Biof100 + trade
Biof100 + area

Figure 4

mio ha	Biof100		Biof100 + trade		Biof100 + area	
	Total cropland	Bioenergy	Total cropland	Bioenergy	Total cropland	Bioenergy
2005	1417.4	40.4	1408.2	45.1	1465.7	41.9
2015	1392.1	64.2	1384.6	68.0	1491.6	70.1
2025	1354.7	101.0	1348.5	103.3	1505.0	114.2
2035	1298.9	155.3	1302.6	148.8	1496.6	179.4
2045	1219.3	233.6	1230.0	220.1	1457.3	276.1
2055	1105.4	345.3	1123.6	325.4	1369.3	421.1

Figure 5

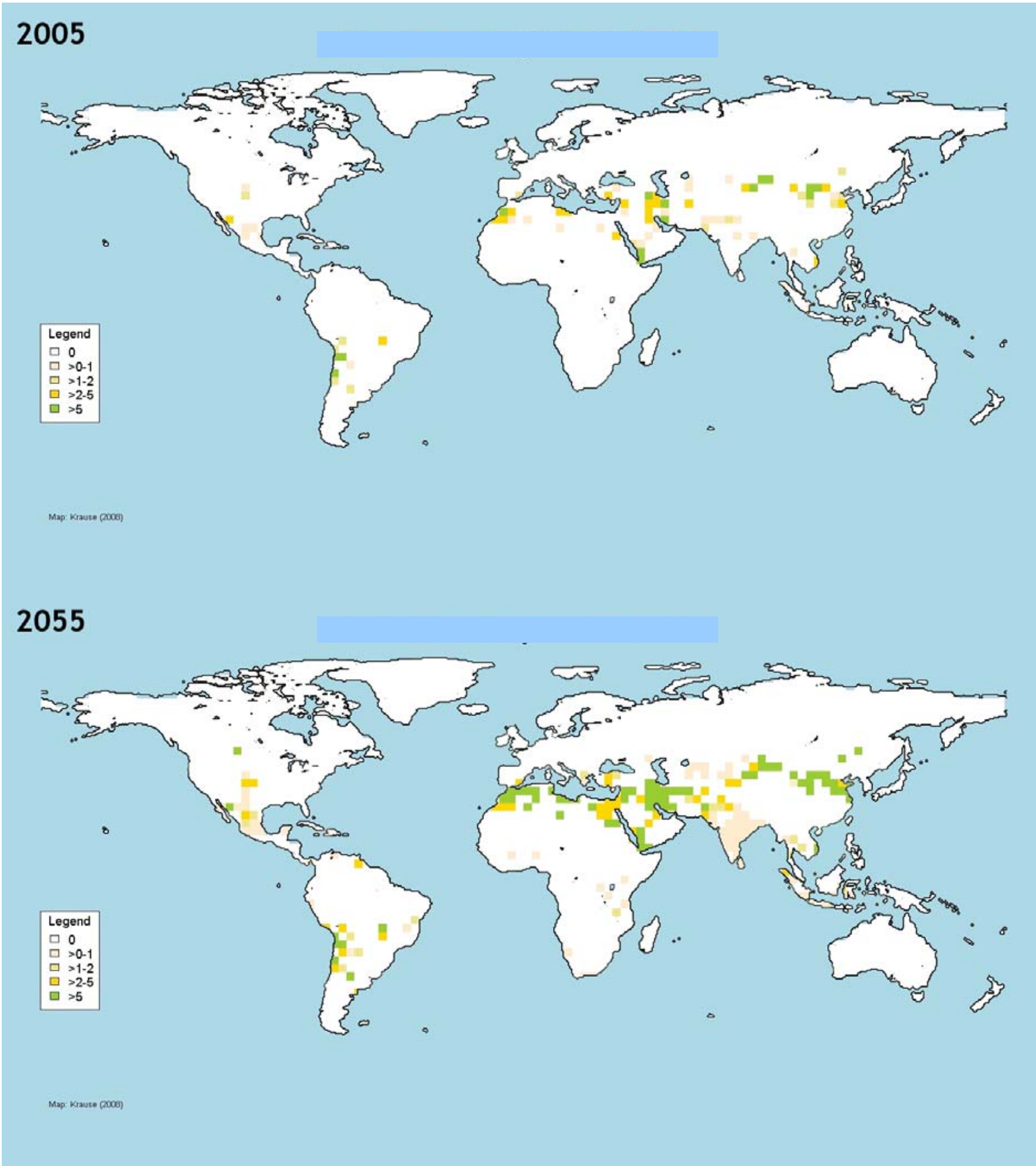
2005
Legend
0
>0-1
>1-2
>2-5
>5
Map: Krause (2008)
2055
Legend
0
>0-1
>1-2
>2-5
>5
Map: Krause (2008)

Figure 6

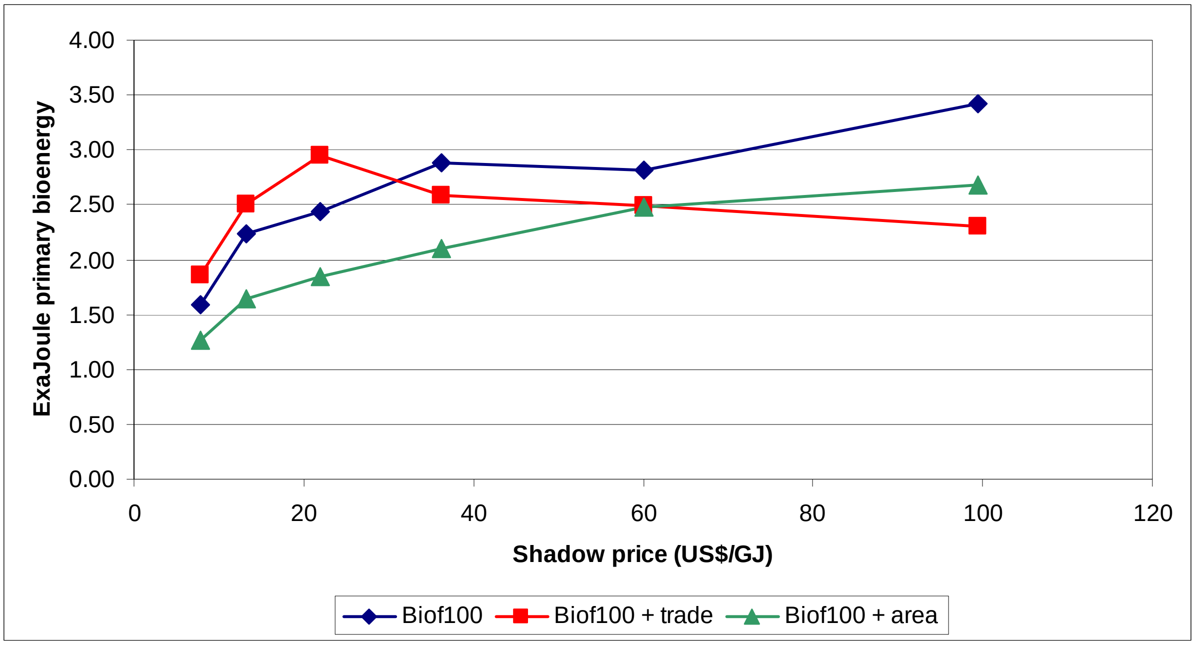
4.00
3.50
3.00
2.50
2.00
1.50
1.00
0.50
0.00
ExaJoule primary bioenergy
0
20
40
60
80
100
120
Shadow price (US$/GJ)
Biof100
Biof100 + trade
Biof100 + area